Available online at www.sciencedirect.com
ScienceDirect
C. R. Geoscience 339 (2007) 840–848
COMPTES RENDUS GEOSCIENCE
http://france.elsevier.com/direct/CRAS2A/

Tectonics

A model for fracturation in the Loyalty Islands

Igor Bogdanov [a,b], David Huaman [c,1], Jean-François Thovert [b], Pierre Genthon [d,2], Pierre M. Adler [a,*]

[a] *UPMC Sisyphe, 75252 Paris cedex 05, France*
[b] *LCD/PTM, 86962 Futuroscope cedex, France*
[c] *IRD/Espace, département de géographie, université d'Orléans, 10, rue de Tours, B.P. 46527, 45072 Orléans cedex 2, France*
[d] *IRD/Paléotropique Nouméa, B.P. A5 98848, New Caledonia*

Received 7 January 2007; accepted after revision 24 September 2007
Available online 19 November 2007

Presented by Jean Aubouin

Abstract

The Loyalty Islands are a series of limestone karstified islands that are currently uplifted and deformed on the elastic bulge of the Australian plate before its subduction at the Vanuatu trench (SW Pacific). These islands have been extensively surveyed for geology and hydrogeology, and fracturation maps have been produced which indicate a major direction N110 ± 35°. This fracture orientation is analytically modeled as resulting from the elastic deformation of the Australian lithosphere before its subduction. First, the vertical deflection around a circular subduction zone is determined. Second, a point force is introduced which accounts for the first stages of a collision between the Loyalty ridge and this circular subduction zone. This model yields principal stress orientations and elevations of the islands in fair agreement with real data. ***To cite this article: I. Bogdanov et al., C. R. Geoscience 339 (2007).***

Résumé

Un modèle pour la fracturation dans les îles Loyauté. Les îles Loyauté sont une série d'îles calcaires karstifiées, qui sont soulevées et déformées au cours de leur montée sur le bourrelet élastique que forme la plaque Australie, avant sa subduction dans la fosse des Vanuatu (Pacifique sud-ouest). La géologie et l'hydrologie de ces îles ont été étudiées de manière extensive et des cartes de fracturation indiquent une direction majeure N110 ± 35°. L'orientation des fractures a été modélisée analytiquement comme le résultat de la déformation élastique de la lithosphère australienne avant la subduction. La déflection verticale autour d'une zone de subduction circulaire a été déterminée. De plus, les premières étapes de la collision entre la ride des Loyauté et cette zone de subduction circulaire ont été prises en compte par une force ponctuelle. Ce modèle fournit des directions de contraintes principales et des élévations des îles en bon accord avec les observations. ***Pour citer cet article : I. Bogdanov et al., C. R. Geoscience 339 (2007).***

Keywords: Fracturation; Subduction; Elastic plate; South-West Pacific; Coral island

Mots clés : Facturation ; Subduction ; Plaque élastique ; Sud-Ouest Pacifique ; Île corallienne

* Corresponding author.
E-mail address: padler@ccr.jussieu.fr (P.M. Adler).
[1] Present address: UNAMBA, Arenas 121, Abancay, Apurimac, Peru
[2] IRD Hydrosciences, case MSE, université Montpellier-2, place Eugène-Bataillon, 34095 Montpellier cedex 5, France

1631-0713/$ – see front matter
doi:10.1016/j.crte.2007.09.012

1. Introduction

The Australian plate is subducting under the Pacific plate at the Vanuatu trench since the Middle Miocene [4]. This plate presents a series of parallel submarine ridges (Fig. 1) including the main island of New Caledonia, and the Loyalty ridge. Cluzel et al. [7] propose that the latter could represent a volcanic arc active before the obduction of ophiolithes onto New Caledonia. It includes a series of Oligocene volcanic seamounts and guyots [20] and four uplifted islands, Ouvéa, Lifou, Maré and Walpole, from northwest to southeast. These islands are thought to be of volcanic origin, but the nature of their basement is still unknown [20], although one outcrop of alkaline Miocene basalt is reported in the middle of Maré [1,18]. The four islands are topped with coral and lagoon-type limestone formations developed during the subsidence of the underlying volcanoes. Coral formations stricto-sensu form cliffs and terraces at the border of the islands, while their inner part consists of non-cohesive lagoon-type biomicrites [5,18]. Walpole is thought to be only a remnant of a larger atoll.

These islands are uplifted to an approximately 130-m altitude during their motion toward the Vanuatu trench. This has been interpreted by Dubois et al. [9,10] as the result of their advance on the elastic bulge developing on the Australian subducting plate before its bending toward the Vanuatu trench. Ouvéa is uplifted at a 40-m altitude in its western part, while its eastern part is still an atoll at sea level. The top of the elastic bulge is located between Lifou and Maré, which culminate at 100 m and 130 m, respectively, while Walpole lies at a 70-m altitude on the trenchward flank of the bulge.

Convergence along the Vanuatu subduction zone is constrained by focal mechanisms of earthquakes and by GPS measurements between the islands of Vanuatu, the Loyalty Islands and the Grande Terre, which is the main island of New Caledonia [3,21]. The convergence rate is 12 cm/yr northward of Ouvéa, Lifou and Maré, and only 4.8 cm/yr along the southern arc. The change of convergence style occurs 100 km southeast of Maré, at the 22° S latitude and is associated in the back-arc with the westward motion of the Mattews-Hunter block (Fig. 1) marked by a senestrial strike-slip seismicity [17]. The deformation recorded in the marine sediments of the back-arc led Monzier et al. [20] to propose that the collision between the Vanuatu arc and the Loyalty ridge occurred 300 000 yr ago.

Measurements of the fissure networks developed inside the limestone material of these islands were one of the topics of the SAGE project (2002–2005) devoted to an assessment of the water management policy in the Loyalty Islands [16]. This project was funded by the New Caledonian Province of Loyalty Islands (PLI), the University of New Caledonia (UNC) and IRD. A fracturation study has been undertaken in Lifou, Ouvéa and Maré Islands, based on teledetection and field studies [13]. As fissures, faults or joints can hardly be observed in the inner part of the islands, since they are largely covered by forests and due to the non-cohesive nature of their superficial layer, this work provides a unique opportunity to compare linear structures deduced from teledetection with the tectonics and geodynamics of this active region.

It is now currently admitted [23] that the oceanic lithosphere can be modeled as an elastic beam (or plate) on which seamounts and subduction zones are acting as loads. This model has been extended by including plasticity (e.g., [19]) and the earth sphericity (e.g., [12]). Thus, the present work will use the fissure network deduced from teledetection to constrain the mechanical state of the Australian lithosphere, assuming that it behaves as a thin elastic plate submitted to various loads and forces.

This article is organized as follows. The data gathered from aerial, satellite and field trips are first presented and analyzed. Then, an elastic 3D model around a circular trench accounting for the curvature of the trench is derived. It includes a vertical deflection under loads distributed along the trench axis and a localized force, corresponding to the ongoing collision of the Loyalty ridge with the Vanuatu subduction zone. Finally, the resulting stress distributions are compared to the fracture data observed in the Loyalty Islands.

2. Field data

The fracturation study involved interpretation of SPOT3 and SPOT4 images, of ENVISAT radar images [13] and of aerial photographs available at the *Direction de la topographie et des transports terrestres* (DI3T) of New Caledonia, which provide a coverage of the islands on a scale of approximately 1/10 000. An extensive field campaign in 2002 and numerous shorter field trips during our hydrological measurement campaigns in Lifou allowed us to check that the lineaments present on the various images were also observed at the outcrop on the coral formations bordering the islands.

However, due to the extensive dissolution of fracture walls induced by rainwater in the tropical climate, fault slip measurements were impossible. Moreover, displacement observations on coral terraces may be misleading, due to the numerous collapses of caves formed by mixing corrosion near the coast [24] and

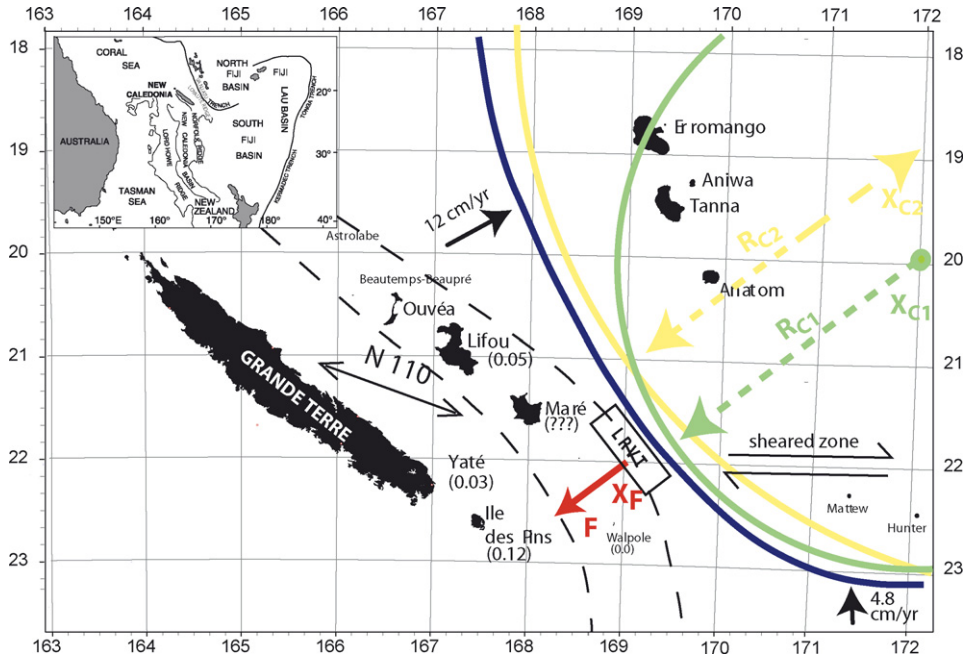

Fig. 1. General geological setting. Tectonic setting (main figure) and localization of the study area (inset). The long dashed lines define the extension of the Loyalty ridge. The axis of the Vanuatu trench is in blue. The convergence rates along the trench are indicated by the heavy arrows (after Calmant et al., [3]). The mean N110 orientation (equivalent to $\theta = -20°$) recorded in the Loyalty Islands is also displayed. The present-day uplift rates are indicated between parentheses (in mm/yr); they are not known in Maré. The box labelled LRVT is the area of the begining collision between the Loyalty ridge and the Vanuatu trench (Monzier et al., [20]). The two circles C_1 and C_2 used to fit the trench shape are indicated in green and yellow, respectively. The positions of their centers (X_{C1} and X_{C2}) and their radii (R_{C1} and R_{C2}) are also indicated. The localized force used to model the collision is displayed in red.

Fig. 1. Contexte géologigue général. Contexte tectonique (figure principale) et localisation de la zone d'étude (en insertion). Les pointillés longs définissent l'extension de la ride des Loyauté. L'axe de la fosse des Vanuatu est en bleu. Les taux de convergence le long de la fosse sont indiqués par les flèches épaisses (d'après Calmant et al., [3]). L'orientation moyenne N110 (équivalente à $\theta = -20°$) mesurée dans les îles Loyauté est également représentée. Les taux de soulèvement actuels en mm/an sont indiqués entre parenthèses ; ils ne pas connus pour Maré. La boîte notée LRVT est la zone de collision commençant entre la ride des Loyauté et la fosse des Vanuatu (Monzier at al., [20]). Les deux cercles C_1 et C_2 utilisés pour schématiser la fosse sont indiqués en vert et en jaune. Les positions de leurs centres (X_{C1} et X_{C2}) et leurs rayons (R_{C1} et R_{C2}) sont également indiqués. La force ponctuelle utilisée pour modéliser la collision est représentée en rouge.

possible reworking of rock blocks by hurricanes. Due to the dense vegetal cover inside the islands, fractures are hardly observed except inside quarries, where the lagoon-type biomicrite, extensively dissolved, recristallized and partly dolomitized generally presents a non-cohesive facies [18]. Hence, fractures or discontinuities can be hardly observed in the inner part of the island.

Owing to the great difficulty of observing fractures and fracture displacements in these islands, it was concluded that it was better to work only with the lineaments observed by teledetection. These lineaments were termed as fractures, altough they may represent joints, faults or any kind of linear structure. Preliminary and final versions of the fracture maps have been published by Maurizot and Lafoy [18] and Huaman [13], respectively.

In the original maps, each fracture was replaced by the segment joining its two extremities, and the segment orientations θ were measured in degrees with the standard trigonometric convention (Fig. 2 a). Orientation histograms in length of these maps were built (Fig. 2b).

Because of the presence of two local maxima around the main one (Fig. 2), the fractures were decomposed into three families F1, F2 and F3 fitted by Gaussian distributions:

$$\text{Fi family}: \quad k_i \exp\left[-\frac{(\theta - m_i)^2}{2\sigma_i^2}\right], \; i = 1, 2, 3 \qquad (1)$$

where the subscript i denotes the families. m_i is the average angle, σ_i the standard deviation and k_i is expressed in meters of fracture traces per km^2 and per degree. The values of these parameters are given in Table 1. The fit, Eq. (1), is rather satisfactory (see Fig. 2b) and it can be noticed that the families F1 and F3 are oriented at 45 degrees from family F2, which suggests that F1 and F3 are conjugated to F2. The local orientations were analyzed within Lifou divided into

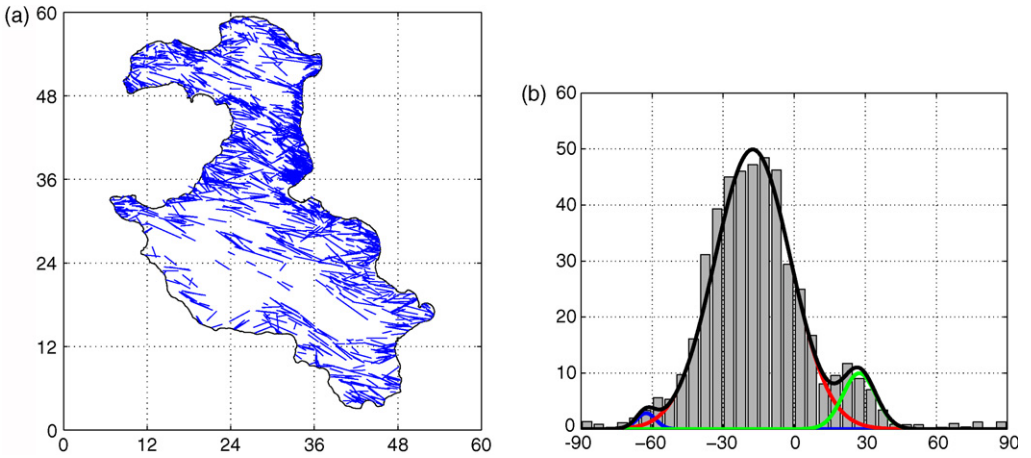

Fig. 2. Fracture map in the Lifou island: (a) each recorded fracture is represented by an end-to-end segment; (b) decomposition of the length-weighted orientation histogram.

Fig. 2. Carte de fracturation dans l'île de Lifou : (a) chaque fracture est représentée par le segment qui joint ses extrémités ; (b) décomposition de l'histogramme des orientations, pondéré en longueur.

5×5 zones of 12×12 km^2, but no obvious systematic evolution was noticed.

The same analysis was performed for Maré and Ouvéa with similar overall results (Table 1). m_i varies slightly, since it is equal to $-15°$, $-17.5°$ and $-20°$ for Ouvéa, Lifou and Maré, respectively. The values of σ_i remain of the same order of magnitude, since the orientations are distributed in a rather symmetric way around the mean orientation within an angle of $\pm 60°$. Even the intensities of fracturation for the three families, quantified by k_i in (1), are remarkably stable. The overall average direction is equal to $-19°$.

However, the length histogram of Ouvéa is qualitatively different from that of Fig. 2 b; roughly speaking, the orientations are uniformly distributed between -40 and $+30°$ with a superposed peak at $0°$.

The fracture orientations deduced from this analysis should be compared to those usually recorded in this region. Lagabrielle et al. [15], and Chardon and Chevillotte [6] compiled previous tectonic studies on Grande Terre and its region; Lafoy et al. [14] and Flamand et al. [11] studied submarine deformation. The first obvious discontinuity direction is that of the Loyalty ridge ($-40°$), which is also recorded as an extensive fault direction along Grande Terre, and does not fit any of the observed fracture orientations. However, the $-65°$ direction corresponds well to that of the trench in the area and is recorded as a secondary fracture orientation in Grande Terre. Lafoy et al. [14] reported a WSW–ENE trend in the submarine Loyalty ridge interpreted as a recent left lateral strike-slip motion, which could be similar to our $+30°$ orientation. The $-20°$ direction was recorded as an extensional one by Flamand et al. [11] in the submarine terraces bordering the Caledonian lagoon.

The present state of stress in the area is known from focal mechanisms of earthquakes which are mainly located in the bending zone of the Australian plate. As expected on a bending plate, these mechanisms are extensive with the principal extension axis pointing toward the trench [17,21]. The Loyalty Islands are largely aseismic except for the surroundings of

Table 1
The fracture density k_i expressed in meter of fracture traces per square kilometer and per degree, the average angle m_i and the standard deviation σ_i for the three families F1, F2 and F3, and the three islands

Tableau 1
Densité k_i, exprimée en mètre, de traces de fracture par kilomètre carré et par degré, angle moyen m_i et écart-type s_i pour les trois familles F1, F2 et F3, et pour les trois îles. Les trois dernières lignes correspondent aux moyennes générales

Parameters	k_i	m_i (°)	σ_i (°)
Ouvéa			
F1	7.0	−60	6
F2	47.7	−15	19
F3	20.1	+30	8
Lifou			
F1	2.9	−62.5	4
F2	49.9	−17.5	16
F3	10.0	+27.5	7
Maré			
F1	4.9	−65	6
F2	51.7	−20	17
F3	15.0	+25	10
Average			
F1	4.0	−64	6
F2	50.4	−19	16.5
F3	12.4	+26	8

The last three lines correspond to the general averages.

Walpole, near the collision zone, where several seismic swarms, reaching $M = 7.2$, have been recorded and for which no focal mechanism has been published so far [22]. Thus, the major fracture orientation of the Loyalty Islands ($-20°$) cannot be considered as an ubiquitous discontinuity direction for the region. This leads us to compare the results of some elastic beam models with these fracture patterns.

The tectonic situation can be simplified as follows. The Loyalty Islands are located in the immediate neighbourhood of a subduction zone which can be approximated by circles (Fig. 1). Moreover, the relative velocity between the two plates almost vanishes at the latitude 22° S. This suggests that the first stages of the collision between the Loyalty ridge and the Vanuatu trench zone (LRVT in Fig. 1) induce a stress distribution that is modeled here as a single force. This force represents the integration ot the stress distribution over the whole LRVT zone. It is assumed to be applied at the middle of the LRVT zone, at 22° S, 169° E. The cases of a radial (perpendicular to the trench axis) and of an east–west force are considered. The radial force corresponds to the assumption that no shear stress can be transmitted at the trench, while the east–west force corresponds to the strike slip decoupling motion inferred in the back-arc domain by Monzier et al. [20] and Lafoy et al. [14] (see Fig. 1).

This simplified image of the real situation is illustrated by Fig. 1. The Vanuatu subduction zone is replaced by a circle of center $\boldsymbol{X}_C$ and radius R_C. The Australian and the Pacific plates correspond to the regions outside and inside this circle, respectively. The stresses due to this particular situation are caused partly by the vertical deflection of the elastic Australian plate at the Vanuatu subduction zone, and partly because of the force $\boldsymbol{F}$.

3. Theory

Basically, the theoretical model considers an elastic thin plate submitted to a load at the subduction zone schematized by a circle and to an horizontal force caused by the collision between the Loyalty ridge and the Vanuatu trench zone.

3.1. Deformation of a lithospheric plate surrounding a circular ocean

Consider the vertical deflection W of a lithospheric plate of thickness h under a vertical load which surrounds a circular hole of radius R_o as depicted in Fig. 1. The load can be decomposed into the weight of the plate $\rho_m g$ (where ρ_m is the density of the plate and g the acceleration of gravity) and the hydrostatic force exerted by water, whose density is ρ_w. This generalizes the one-dimensional calculations given by Turcotte and Schubert [23]. The characteristic length α_e is called the flexural parameter:

$$\alpha_e = \left[\frac{Eh^3}{12(1-\nu^2)(\rho_m - \rho_w)g}\right]^{1/4} \tag{2}$$

where E is the Young modulus and ν the Poisson ratio.

Let us introduce the dimensionless lengths r and w:

$$r = \frac{R}{\alpha_e}, \quad w = \frac{W}{\alpha_e} \tag{3}$$

w is governed by a biharmonic equation further simplified by the assumption of cylindrical symmetry:

$$\frac{1}{r}\frac{\mathrm{d}}{\mathrm{d}r}\left[r\frac{\mathrm{d}}{\mathrm{d}r}\left\{\frac{1}{r}\frac{\mathrm{d}}{\mathrm{d}r}\left(r\frac{\mathrm{d}w}{\mathrm{d}r}\right)\right\}\right] + w = 0 \tag{4}$$

together with the boundary conditions at infinity:

$$w = 0, \quad \frac{\mathrm{d}w}{\mathrm{d}r} = 0 \text{ at } r = \infty \tag{5}$$

The general solution can be written as:

$$w(r) = A.\,\mathrm{Re}\{K_0(\rho)\} + B.\,\mathrm{Im}\{K_0(\rho)\} \tag{6}$$

where K_0 is the zero order modified Bessel function of the second kind. This solution is similar to the classical one (e.g. Watts, [25]) of a point load acting on a circular plate. The two constants A and B need to be determined from the boundary conditions at $r = r_0$. The procedure used by Turcotte and Schubert [23] is transposable to the circular case. A and B are expressed as functions of the radius r_m corresponding to the maximal deflection w_m and of the radius r_1 corresponding to $w = 0$. This requires some easy, but cumbersome algebra which is not detailed.

The stresses $\boldsymbol{\sigma}^D$ at the upper surface of the plate can be derived from this solution and made dimensionless by the characteristic stress σ_{SD}:

$$\boldsymbol{\sigma}^{D*} = \frac{\boldsymbol{\sigma}^D}{\sigma_{SD}}, \quad \sigma_{SD} = \frac{6D\mathrm{w}_{\max}}{(\alpha_e h)^2} \tag{7}$$

3.2. Deformation of a lithospheric plate under an horizontal localized force

Consider now a localized horizontal force applied onto the plate along a vertical segment of two-dimensional coordinates $\boldsymbol{X}_F$ as illustrated in Fig. 1.

Let $\boldsymbol{F}$ be the force exerted per unit length. It is more convenient to introduce other units of length R_o, and force $R_o\|\mathbf{F}\|$. The stresses verify:

$$\boldsymbol{\sigma}^F = \frac{F_o}{R_o^2}\boldsymbol{\sigma}^{*F} \tag{8}$$

The solution to this problem can be found using a complex variable formalism for plane isotropic elasticity in which the solutions are given by two analytic functions $\phi(z)$ and $\psi(z)$ of a complex variable $z = x + iy$. The solution for an elliptical hole was given by Denda and Kosaka [8].

3.3. Superposition of the two solutions

When the deflection and the point force are superposed, the dimensionless resulting stress Σ^* can be defined as:

$$\Sigma^* = \frac{\Sigma}{\sigma_{SD}} = \boldsymbol{\sigma}^{D*} + \omega\boldsymbol{\sigma}^{*F} \tag{9a}$$

where the dimensionless parameter ω is given by:

$$\omega = \frac{F_o(\alpha_e h)^2}{6R_o^2 w_{max} D} \tag{9b}$$

4. Comparison with fracturation data

4.1. Altitudes of the Loyalty Islands

The Vanuatu subduction zone (Fig. 1) can be approximated by a circle in two opposite ways. The circle C_1 approximates the southern part of the zone and it does not represent well the northern part of the zone. C_2 provides an approximation to the whole subduction zone, but it is much less precise south of 22° S. These two circles are characterized by the longitude and latitude of their center, and by their radius, namely $C1$ ($\boldsymbol{X}_{C1}$: 172° E, −20° S; $R_{C1} \approx 395$ km) and $C2$ ($\boldsymbol{X}_{C2}$: 173.6° E, −17.55° S; $R_{C2} \approx 670$ km).

Systematic applications of (6) were made with $C1$, $C2$ and $\alpha_e = 50, 70, 100, 140$ km. The main physical parameters are: $E = 7 \times 10^{10}$ Pa, $\nu = 0.25$, $\rho_m = 3.3 \times 10^3$ kg m^{-3}, $\rho_w = 10^3$ kg m^{-3}. The local force $\boldsymbol{F}$ is not taken into account. For a given value of α_e, r_1 is chosen in order to minimize the norm of the difference between W and the observed altitudes of the four Loyalty Islands taken from Dubois et al. [10].

Fig. 3 shows that for $C2$ the elevations of the four islands can be virtually fitted by any of the elastic profiles.

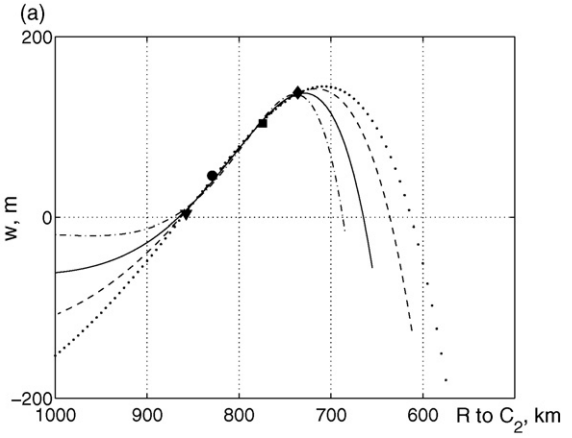

Fig. 3. The dimensional altitude of the Loyalty Islands as a function of the distance to the center $\boldsymbol{X}_{c2}$ of the circle C_2. α_e is equal to: 50 (dash-dot), 70 (solid), 100 (broken), 140 (dotted). The dots correspond to the four Loyalty Islands: from left to right: Beautemps Beaupré, Ouvéa, Lifou and Maré.

Fig. 3. Altitude (m) des îles Loyauté en fonction de la distance au centre $\boldsymbol{X}_{C2}$ du cercle C_2. α_e est égal à 50 (trait mixte), 70 (trait continu), 100 (trait brisé), 140 (trait pointillé). Les symboles correspondent aux quatre îles Loyauté ; de gauche à droite : Beautemps Beaupré, Ouvéa, Lifou et Maré.

Since the reef westwards of Beautemps Beaupré does not show any uplift, a value of α_e ranging between 50 and 70 km should be adopted for $C2$. Basically, the same conclusions hold for $C1$, which is not shown here. These values are very similar to the one found by Dubois et al. [10], i.e. 58 ± 2 km, which corresponds to an elastic thickness of 22 km. According to these authors, this elastic thickness is lower than the 28-km thickness expected for the 50-Myr age of the oceanic lithosphere deduced from magnetic anomalies, but is consistent with a thermal age of 25 Myr deduced from the mean depth of the Loyalty basin. Burov and Diament [2], using a larger data set, showed in their Fig. 1 that the elastic thickness of a 50-Myr-old oceanic lithosphere should be around 34 km, when deduced from deformations at trenches or at fracture zones only, i.e., if seamounts possibly associated with thermal effects are discarded. A 25-Myr oceanic lithosphere is generally too young to enter in subduction and, therefore, there is no trench data for its elastic thickness. These remarks reinforce the hypotheses of Dubois et al. [10] that the Loyalty basin lithosphere has been rejuvenated by the thermal events associated with the emplacement of the Loyalty ridge seamounts.

4.2. Stress intensities and orientations

The values of the maximal compression and extension denoted by Σ_1 and Σ_2, respectively, were

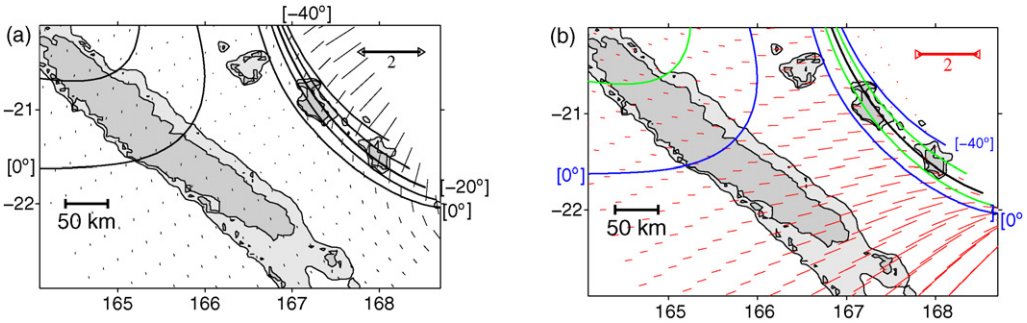

Fig. 4. The maximal extension Σ_2 (a) and compression Σ_1 (b) for the superposed fields for the circle C_2. The data are the principal components of the dimensionless stress tensor Σ^* in (9a), for a radial force, applied at ($\phi_f = 169.5°$ E, $\theta_f = -22.2°$ S). Data are for $\alpha_e = 45$ km, $R_m = \alpha_e r_m = 716$ km, $R_1 = 670$ km, $\omega = 0.025$. The lines correspond to isodirections of the perpendicular to the largest extension (i.e., parallel to the fracturation): $0, -10, -20, -30, -40°$. The thick black line (in b) corresponds to $-20°$ which is close to the average found for the three Loyalty Islands. The stress scale is indicated by the bar in the top-right corners; 1 corresponds to 68 MPa.

Fig. 4. Extension maximale Σ_2 (a) et compression maximale Σ_1 (b) pour les champs superposés pour le cercle C_2. Les résultats sont les composantes principales du tenseur des contraintes adimensionnel Σ^* dans (9a), pour une force radiale appliquée en ($\phi_f = 169.5°$ E, $\theta_f = -22.2°$ S). Les résultats correspondent à $\alpha_e = 45$ km, $R_m = \alpha_e r_m = 716$ km, $R_1 = 670$ km, $\omega = 0.025$. Les lignes correspondent aux isodirections de la perpendiculaire à l'extension maximale (c'est-à-dire parallèle à la fracturation): $0, -10, -20, -30, -40°$. La ligne noire épaisse (en b) correspond à $-20°$, ce qui est proche de la moyenne obtenue pour les trois îles Loyauté. L'échelle des contraintes est indiquée par la barre dans les coins supérieurs droits ; 1 correspond à 68 MPa.

calculated by superposing the two elementary solutions. In addition to the previous parameters, the force orientation and its intensity (i.e., ω) were systematically studied. The force was chosen to be either radial or east–west. ω plays the role of an adjustable parameter in order to orient the direction of Σ_2 perpendicular to the average fracture direction $m = -20°$.

When comparing modeled stresses and actual fracture sets observed in the islands, it should be kept in mind that: (*i*) at the outrop, these discontinuities appear as craks or joints with centimetric or no offset; and (*ii*) superficial (low confining pressure) deformation only is observed, since the thickness of the limestones may be estimated at less than 200 m. Therefore, crack opening is assumed to occur under tension only, as it is well suited to near surface deformation. This implies that fractures are parallel to the compression direction in Fig. 4.

The systematic results can be summarized as follows. For C_1, the influence of α_e and of the direction of $\boldsymbol{F}$ on the directions and intensities of the stresses is weak. Moreover, the stress directions hardly vary over the islands and this would imply a very well defined fracture direction.

Another possible criterion is the relative intensity of Σ_1 and Σ_2. In order that rupture occurs preferentially perpendicular to the extensive stress, Σ_2 should be comparable to Σ_1. This is generally not true for C1.

The results for C2 are very different. The influence of α_e on the directions and intensities of the stresses is strong for a radial force and much weaker for an east–west force. The influence of the direction of the force is stronger for $\alpha_e = 45$ km than for 70 km. These stronger influences are probably due to the fact that C_2 is closer to the islands than C_1.

A remarkable combination of parameters was found for C2 and it is displayed in Fig. 4, where the unit for the dimensionless stresses is 68 MPa. Σ_2 is perpendicular to $-20°$ over Maré and Lifou and the angle variations over these islands are very large when compared to those obtained for the other combinations of parameters. This is in good agreement with the observed orientations in these two islands which are mostly ranging between -50 and $20°$ (Fig. 2). Moreover, Σ_1 is of the order of Σ_2.

Because of its linear shape, Ouvéa is a special case and Fig. 4 a predicts that the fractures should be oriented east–west, i.e., with an angle equal to 0. It is interesting to recall that the Ouvéa length histogram presents an almost uniform distribution between -30 and $+40°$ with a peak at 0°. However, Σ_1 is significantly larger than Σ_2 over Ouvéa.

Moreover, the small drift of the average fracture direction between the three islands, which goes from -15 to $-20°$ from Ouvéa to Maré, can be easily accounted for by the respective situation of these islands with respect to the isodirections of the stresses.

A last important remark is that before the collision of the Loyalty ridge started, Lifou and Maré should have been shifted westward by about 30 km. They were only submitted to the stress regime induced by the subduction of the Australian lithosphere. This should have induced an extensive stress regime associated with

the aperture of joints directed parallel to the subduction zone, i.e., nearly −60°, which corresponds to one of the minor lobes of the fracture distributions (see Table 1).

5. Concluding remarks

A partially analytical study has been carried out in order to relate the fracturation observed on the Loyalty Islands to the deformation of the Australian lithosphere due to its subduction. A novel solution is given to subduction around a circular plate in terms of Bessel functions. A classical point force solution is superposed to it.

The altitudes of the Loyalty Islands and the observed fracture orientations are in agreement with the solution presented here. Moreover, the order of magnitude of stress intensities are in the range of acceptable values. Finally, this solution implies a large dispersion of fracture orientations which is indeed observed and which could be hardly accounted by with a single tectonic phase with well-defined stress orientations. Indeed, the model presented here may not be the unique solution to explain the fracture distribution observed in the Loyalty Islands. In particular, if the −20° orientation is a major anisotropy direction of the basement of the islands, it may be reactivated by a large class of tectonic events. Until now, this direction has never been proposed for the Loyalty ridge, although it is known as a recent tectonic direction in Grande Terre [11]. The model is consistent with the thin elastic plate theory currently admitted for the oceanic lithosphere and it is able to reproduce the observations. This model does not require any refinement of the rheological profile of the lithosphere. However, a good fit of the fracturation data cannot be obtained without a force describing the interaction between the Loyalty ridge and the Vanuatu trench. This implies that the collision involves the whole lithosphere thickness and is not restricted to the superficial sediment layer.

In the future, the stress orientations computed from this model will be compared with the drainage directions in the karstified Loyalty Islands. In addition, stress intensities could help to assess seismic hazards. This would probably require a numerical study which would take into account the real shape of the subduction zone.

Acknowledgments

Most computations were performed at CINES (subsidized by the MENESR). This work was also partly supported by PNRH, which is gratefully acknowledged. Dominique Cluzel is also thanked for his participation in the field work and for valuable discussions.

References

[1] J.C. Beaubron, J.H. Guillon, J. Récy, Géochronologie par la méthode K/Ar du substrat volcanique de l'île de Maré, archipel des Loyauté (Sud-Ouest Pacifique), Bull. BRGM 4 (1976) 165–176.

[2] E.B. Burov, M. Diament, The effective elastic thickness of continental lithosphere (Te): what does it really mean? J. Geophys. Res. 100 (1995) 3905–3927.

[3] S. Calmant, B. Pelletier, P. Lebellegard, M. Bevis, F.W. Taylor, D.A. Phillips, New insights on the tectonics along the New Hebrides subduction zone based on GPS results, J. Geophys. Res. 108 (2003) 2319, doi:10.1029/2001JB000644.

[4] J.N. Carney, A. Macfarlane, Geological evidence bearing on the Miocene to recent structural evolution of the New Hebrides Island Arc, Tectonophysics 87 (1982) 147–175.

[5] D. Carrière, Enregistrement sédimentaire, diagénétique et morphologique d'un bombement de la lithosphère sur l'atoll soulevé de Maré, Nouvelle Calédonie, C. R. Acad. Sci. Paris, Ser. II 306 (1987) 975–980.

[6] D. Chardon, V. Chevillotte, Morphotectonic evolution of the New Caledonia ridge (Pacific Southwest) from post-obduction tectonosedimentary records, Tectonophysics 420 (2006) 473–491.

[7] D. Cluzel, J.C. Aitchinson, C. Picard, Tectonic accretion and underplating of mafic terranes in the Late Eocene intraoceanic fore-arc of New Caledonia (Southwest Pacific): geodynamic implications, Tectonophysics 340 (2001) 23–59.

[8] M. Denda, I. Kosaka, Dislocation and point-force-based approach to the special Green's function BEM for elliptic hole and crack problems in two dimensions, Int. J. Num. Meth. Eng. 40 (1997) 2857–2889.

[9] J. Dubois, J. Launay, J. Récy, Some new evidences on lithospheric bulges close to island arcs, Tectonophysics 26 (1975) 189–196.

[10] J. Dubois, C. Deplus, M. Diament, J. Daniel, J.-Y. Collot, Subduction of the Bougainville seamount, Vanuatu: mechanical and geodynamic implication, Tectonophysics 149 (1988) 111–119.

[11] B. Flamand, B. Pelletier, G. Cabioch, Y. Lagabrielle, The New Caledonia margin: morphology and tectonics, submitted to Tectonophysics (2007).

[12] Y. Fukao, K. Yamaoka, T. Sakurai, Spherical shell tectonics: buckling of subducting lithosphere, Phys. Earth Planet. Inter. 45 (1987) 59–67.

[13] D. Huaman, Construction de la base de données cartographique et géologique des îles Loyauté ainsi que de leur SIG, Rapport SAGE, IRD et Province des Iles, Nouméa, 2004 (54 p).

[14] Y. Lafoy, F. Missègue, D. Cluzel, R. Le Suave, The Loyalty-New Hebrides arc collision: effects on the Loyalty ridge and basin system, Southwest Pacific (first results of the ZoNéCo Program), Mar. Geophys. Res. 18 (1996) 337–356.

[15] Y. Lagabrielle, P. Maurizot, Y. Lafoy, G. Cabioch, B. Pelletier, M. Regnier, I. Wabete, C. Calmant, Post-Eocene extensional tectonics in southern New Caledonia (SW Pacific): Insights from onshore fault analysis and offshore seismic data, Tectonophysics 403 (2005) 1–28.

[16] D. Lille, M. Allenbach, D. Houmbouy, SAGE Gestion durable de la ressource en eau des Loyautés. Un programme de recherches

scientifiques et technologiques au service du développement, Geologues 138 (2004) 66–68.
[17] R. Louat, B. Pelletier, Seismotectonics and present-day relative plate motions in the New Hebrides, North Fiji Basin region, Tectonophysics 167 (1989) 41–55.
[18] P. Maurizot, Y. Lafoy. Notice explicative, Carte géol. Nouvelle-Calédonie (1/50 000), feuilles Maré, Lifou et Ouvéa, Iles Loyauté. Service des Mines et de l'Energie, Bureau de Recherches Géologiques et Minières, Nouméa, Nouvelle Calédonie, 2003.
[19] M.K. McNutt, H.W. Menard, Constraints on yield strength in the oceanic lithosphere derived from observations of flexure, Geophys. J. Astron. Soc. 71 (1982) 363–394.
[20] M. Monzier, J. Daniel, P. Maillet, La collision ride des Loyauté/arc des Nouvelles Hébrides (Pacifique Sud-Ouest), Oceanol. Acta 10 (1990) 43–56.
[21] B. Pelletier, C. Calmant, R. Pillet, Current tectonics of the Tonga-New Hebrides region, Earth Planet. Sci. Lett. 164 (1998) 263–276.
[22] R. Pillet, B. Pelletier, Tectonique active, tsunamis et sismicité en Nouvelle-Calédonie. Notes Techniques, Sciences de la Terre, Géologie-Géophysique, IRD Nouméa, no. 28, 19 p., 2004. mise à jour 2005.
[23] D.L. Turcotte, G. Schubert, Geodynamic applications of continuum physics to geological problems, John Wiley, New York, 1982.
[24] H.L. Vacher, T.M. Quinn (Eds.), Geology and Hydrogeology of Carbonate Islands, Elsevier, Amsterdam, 1997.
[25] A.B. Watts, Isostasy and flexure of the lithosphere, Cambridge University Press, Cambridge, 2001.